Supporting Information for
Mercury Vapor Release from Broken Compact Fluorescent Lamps and In Situ Capture by New Nanomaterial Sorbents

Natalie C. Johnson, Shawn Manchester, Love Sarin,
Yuming Gao, Indrek Kulaots, Robert H. Hurt

Division of Engineering and Institute for Molecular and Nanoscale Innovation
Brown University, Providence, RI USA

Number of pages: 4

Number of figures: 2

Additional Information on Materials and Methods

Sorbents

Copper, both micro- and nanoscale metal particles, were obtained from Sigma Aldrich (<10 µm) and Alfa Aesar (20-40 nm, 13 m^2/g) respectively. The nano-copper samples were used both immediately after opening the sealed bottles and again after aging in laboratory air for a period of weeks. Accelerated oxidative aging was carried out by heating the copper nanoparticles in air at 350°C for 1 hour in a laboratory tube furnace. Nickel microsized metal powder was obtained from Sigma-Aldrich (~3 µm diameter). Nickel nanoparticles were obtained from Alfa Aesar (15-25 nm, 15.9 m^2/g). Zinc metal powders were obtained from Sigma-Aldrich (microproduct <10 µm and nanoproduct <50 nm, 3.7 m^2/g). Silver nanoparticles were obtained from Inframat Advanced Materials (100-500 nm and 1.2 m^2/g as received). All the metal powders were studied shortly after unpacking unless noted as processed in some way. Microsized molybdenum sulfide and tungsten sulfide powders were obtained from Sigma Aldrich (both <2µm). Tungsten disulfide nanoparticles were obtained from Nanostructured & Amorphous Materials, Inc. (BET area of 30 m^2/g). All the nano-metal samples were used freshly opened except as noted.

Mercury adsorption capacity measurements

Elemental mercury vapor was generated in Ar (300 cc/min) at 60±3 $\mu g/m^3$ using the Hg CAVKIT 10.534 (PS Analytical, Ltd) and passed through a fixed bed of sorbent resting on a

Pyrex fritted disk inside a tubular Pyrex reactor (*1*). The exit Hg concentration was monitored semi-continuously (3.8 min sampling time) by atomic fluorescence using the Sir Galahad II (PS Analytical, Ltd), which was calibrated using a commercial mercury vapor standard that measures the temperature immediately above an internal pool of elemental mercury liquid. Mercury concentration versus time data were recorded and integrated to find the total amount of mercury adsorbed or reacted.

Figure 1 shows an example breakthrough curve arising from the Hg capture experiments. Selected samples were studied in replicate (including nano-S, nano-Se, bulk Se, nano-Ag) and reproducibility of the total capacities are on the order of +/- 20%. Carbon black was a standard sample used to check the total system performance and calibration before the start of a sorbent series. Integrating over time the difference between the inlet concentration (60 ug-Hg/m^3) and the outlet concentration (see Fig. 1) yields a mass of adsorbed mercury, which divided by sorbent mass yields a capacity reported in μg-Hg/g-sorbent in Table 1 of the main manuscript.

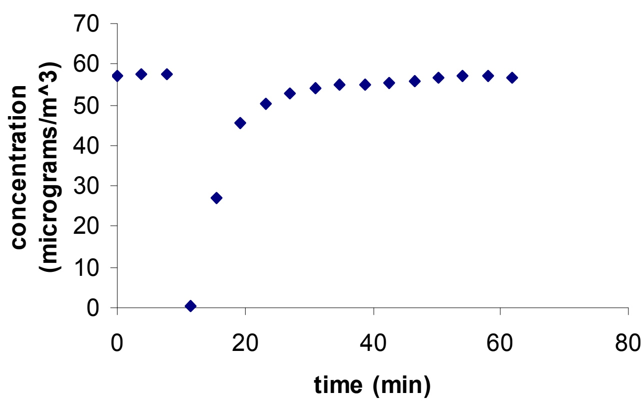

FIGURE 1. Example breakthrough curve in our fixed-bed sorbent evaluation experiments. Time scales range from 20 minutes to 184 hrs depending on specific behavior of the sorbent in question.

The effectiveness of several sorbents in capturing mercury released from fractured CFLs was tested in a proof-of-principle experiment using the flow system discussed above. The CFL was fractured in a flexible 2L Teflon enclosure. The sorbent was distributed into Teflon enclosure in several ways. Sulfur-impregnated activated carbon was added as loose granules. Nano-selenium was applied as a loose powder in a vial, and also as a sorbent patch (a kimwipe covered with nano-selenium) that was placed over the lamp. After lamp fracture, the enclosure was isolated from the flow system for 24 hours. At the end of this period, the enclosure was reintegrated into the flow system, the high purity nitrogen stream was initiated, and the effluent was analyzed for mercury content.

Additional Information on Results and Discussion

Annealing nano-silver reduces both its surface area and Hg capture capacity (see Figure 2 and Hg capacity data in Table 1 in manuscript).

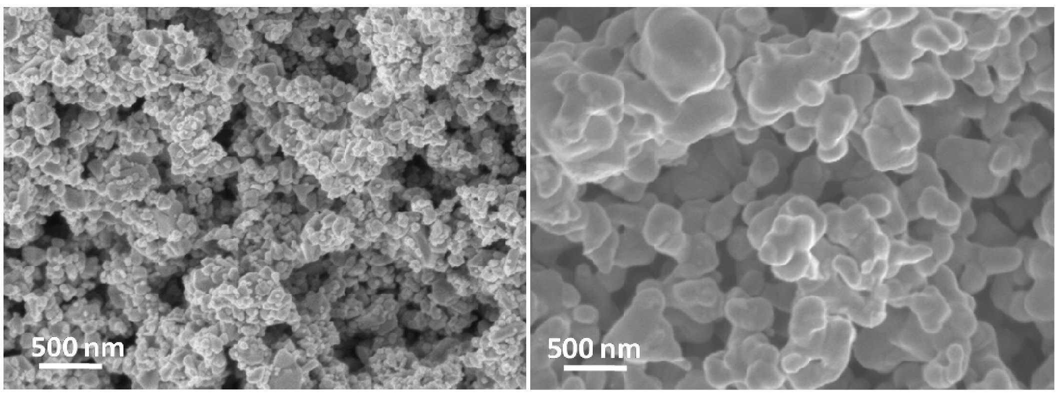

FIGURE 2. SEM images of nano-silver particles before (left) and after (right) vacuum annealing at 500°C.

Additional discussion on health effects of potential sorbents

For consumer applications one must consider the potential health risks of the sorbent in relation to the risk reduction associated with reduced mercury exposure. This is a potential issue with many of the materials and especially nanomaterials in this study, but nano-selenium deserves special comment due to its technological promise. Selenium is an essential trace element (US Recommended Daily Allowance (RDA) of 50 μg/day) and at higher doses a toxicant (No Adverse Effect Level (NOAEL) of approximately 800 μg /day) (*2*). Diets deficient in selenium in some geographic locations have led to selenium supplementation in fertilizer or water supplies (*3*). Human toxicity is rare and affected individuals consumed an average of about 5 mg/day (*3*). The elemental form of selenium is generally regarded as non-bioavailable when taken orally. The

LD50 value of elemental selenium in rats is 6700 mg/kg (*4*), which is a factor of two less toxic than table salt. There is one report (*5*) of an LD50 for stabilized nano-selenium (92.1 mg/kg for mice), indicating a toxicity intermediate between non-toxic bulk elemental form (6700 mg/kg) and selenite (7 mg/kg). Selenium can also pose an environmental risk (see for example Presser (6)). Overall, the small amounts of high-capacity nanoselenium required to suppress vapor release from CFLs (< 10 mg), coupled to the poor bioavailability of the elemental form suggest that nano-Se sorbent health risks can be engineered to be minimal. Further development and testing of the unstabilized nano-Se sorbent is warranted.

Additional Literature Cited

(1) Manchester, S.; Wang, X.; Kulaots, I.; Gao, Y.; Hurt, R. High capacity mercury adsorption on freshly ozone-treated carbon surfaces. *Carbon* **2007**, in press.

(2) Whanger, P.; Vendeland, S.; Park, Y. C.; Xia, Y. Metabolism of subtoxic levels of selenium in animals and humans. *Annals of Clinical and Laboratory Science* **1996**, 26 (2), 99-113.

(3) Raymond, L. J.; Ralston, N. VC. Mercury: selenium interactions and health implications. *SMDJ Seychelles Medical and Dental Journal* **2004**, 7 (1), 72-77.

(4) Cummins, L. M.; Kimura, E. T. Safety evaluation of selenium sulfide antidandruff shampoos. *Toxicology and Applied Pharmacology* **1971**, 20, 89-96.

(5) Wang, H.; Zhang, J.; Yu, H. Elemental selenium at nano size posseses lower toxicity without compromising the fundamental effect on selenoenzymes: Comparison with selenomethionine in mice. *Free Radical Biology & Medicine* **2007**, 42, 1524-1533.

(6) Presser, T.S., The Kesterson Effect, *Environmental Management* **1994** 18 (3) 437-454.